References

[1] Allan, R., "Semiconductor Memories," *Spectrum*, Vol. 12, Aug. 1975, pp. 40-45.

[2] Bowers, D. M., "Systems-on-a-Chip," *Mini-Micro Systems*, Vol. 9, July 1976, pp. 42-48.

[3] Derman, S., "Progress in Gigabit Logic Reported for Superfast Switching Uses," *Electronic Design*, Vol. 24, July 19, 1976, pp. 34-38.

[4] Reddi, S. S. and Feustel, F. A., "A Conceptual Framework for Computer Architecture," *ACM Computing Surveys*, Vol. 8, June 1976, pp. 277-299.

[5] Sykes, D. J., "Protecting Data by Encryption," *Datamation*, Vol. 22, Aug. 1976, pp. 81, 84-85.

[6] Butler, M. K., "Prospective Capabilities in Hardware," *Proceedings, National Computer Conference*, New York, 1976, pp. 323-336.

[7] Chu, Y., "Evolution of Computer Memory Structure," *Proceedings, National Computer Conference*, New York, 1976, pp. 733-748.

[8] Feth, G. C., "Memories: Smaller, Faster, and Cheaper," *Spectrum*, Vol. 13, June 1976, pp. 37-43.

[9] Kelly, J., "The Development of an Experimental Electron-Beam-Addressed Memory Module," *Computer*, Vol. 9, Feb. 1975, pp. 32-42.

[10] Turmail, R. L., "EIA Crystal Ball Shows Trends in Electronics to the Year 2012," *Electronic Design*, Vol. 20, June 22, 1972, pp. 34-36.

[11] Torrero, E. A., "Bubbles Rise from the Lab," *Spectrum*, Vol. 13, Sept. 1976, pp. 29-31.

[12] Amelio, G. F., "Charge-Coupled Devices for Memory Applications," *Proceedings, National Computer Conference*, Anaheim, Calif., 1975, pp. 515-522.

[13] Panigrahi, G., "Charge-Coupled Memories for Computer Systems," *Computer*, Vol. 10, April 1976, pp. 33-41.

[14] Critchlow, D. L., "High Speed MOSFET Circuits Using Advanced Lithography," *Computer*, Vol. 10, Feb. 1976, pp. 31-37.

[15] Hnatek, E., "Chipping Away at Core," *Digital Design*, Vol. 6, July 1976, pp. 31-42.

[16] "Mini-Mini Components," *Time*, Vol. 103, May 6, 1974, p. 97.

[17] Turn, R., *Computers in the 1980's*, Columbia University Press, New York, 1974.

[18] Withington, F. G., "Beyond 1984: A Technology Forecast," *Datamation*, Vol. 21, Jan. 1975, pp. 54-73.

[19] Myers, W., "Key Developments in Computer Technology: A Survey," *Computer*, Vol. 10, Nov. 1976, pp. 48-75.

[20] "Computer Proves Architecture Concept (PEPE)," *Aviation Week and Space Technology*, Oct. 11, 1976, pp. 35-36.

[21] Lea, R. M., "Information Processing with an Associative Parallel Processor," *Computer*, Vol. 9, Nov. 1975, pp. 25-32.

[22] Carlson, E. D., "Graphics Terminal Requirements for the 1970's," *Computer*, Vol. 10, Aug. 1976, pp. 37-45.

Streamtube Analysis of a Hydrogen-Burning Scramjet Exhaust and Simulation Technique

N.A. Talcott Jr.* and J.L. Hunt*

NASA Langley Research Center, Hampton, Va.

CURRENT design philosophy for scramjet-powered hypersonic aircraft results in configurations with the entire lower fuselage surface used as part of the propulsion system.[1] The lower aft-end of the vehicle acts as a high-expansion-ratio external nozzle.[2] At hypersonic velocities, the ram drag and gross thrust are large compared with the net thrust; therefore, extreme care must be taken in designing the external nozzle in order to optimize the thrust and lift while minimizing moments that could result in large airplane trim drag penalties and possible instabilities.

The scramjet hydrogen/air combustion products exhaust plume is characterized by embedded and intersection shocks, expansion fans, wakes, reacting gases, and high temperatures.[3] An understanding of these phenomena must be acquired, and design methods must be developed before this type of engine/airframe integration concept becomes a viable hypersonic system. The strong coupling between the propulsion system and aerodynamics of the aircraft makes a simulation of the hydrogen-burning scramjet exhaust imperative for both nozzle design and aerodynamic force data acquisition. NASA Langley has pursued an extensive scramjet/airframe integration R&D program for several years, and has recently developed a promising technique for simulation of thermally perfect scramjet exhaust flows (molecular weight changes less than 2% throughout the flow) using freon/argon gas blends in equilibrium expansions from total temperatures near 500 K (Ref. 3). Freon/argon blends were selected because contractual studies have shown that they can match the ratios of thermodynamic properties (mainly specific heat ratio γ) of the combustion products permitting a simulation at a much lower temperature level.[4] This Note presents the results of a study to determine if this simulation technique can be extended to more complicated flows approaching the complexity of the actual exhaust flow. An analysis is made to determine the state of the flow and the accuracy of the substitute gas simulation in the presence of a shock discontinuity.

Analysis Methods

A one-dimensional finite-rate analysis was used to determine the actual state (equilibrium, finite-rate, or frozen) of a 2-D scramjet nozzle flow. Conditions representative of Mach 6 and 8 cruise flight ($\phi = 1$ and a dynamic pressure range $2.4 \times 10^4 - 7.2 \times 10^4$ N/m^2) were examined. The explicit finite-difference nozzle code of Ref. 5, employing an average γ, ideal-gas expansion was used to compute streamtubes for these two flight conditions. Earlier calculations for these conditions have shown that the assumption of an average γ, ideal gas does not alter the flow significantly.[3] Area distributions were obtained for equilibrium and frozen expansions and found to be almost identical. It has been assumed that the finite-rate area distribution will be bounded by the equilibrium and frozen distributions; therefore, the frozen area distribution was used in the computations. The finite-rate streamtube code of Ref. 6 was used with the selected area distribution to compute equilibrium, frozen, and finite-rate expansions.

In the finite-rate streamtube code, the chemistry modes were expanded in a finite-rate process, while the vibration modes remained in equilibrium. Subsequent calculations with a finite-rate vibrational streamtube code[7] indicate that the nonequilibrium vibrational energy in the nozzle expansions at any point is less than 10% of the total internal energy of the flow. Therefore, the treatment of the vibrational energy, as in equilibrium, is an acceptable assumption for the purpose herein, since the associated distortion of the flow structure is extremely small.

Results and Discussion

The results that follow are presented for a nominal streamtube that essentially provides the correct area distribution for a Mach 6 flight case. Initially, two streamtubes for this flight condition were analyzed, one representing the narrow flowfield region near the nozzle wall, and the other representative of the flowfield region from the wall to the center of the flowfield. The static pressure and temperature distributions for both streamtubes are presented in Fig. 1, where all quantities are nondimensionalized by the conditions at the nozzle entrance (subscript 3). Since the

Received March 7, 1977; revision received April 14, 1977.

Index categories: Simulation; Supersonic and Hypersonic Flow.

*Aero-Space Technologists, Hypersonic Aerodynamics Branch, High-Speed Aerodynamics Division.

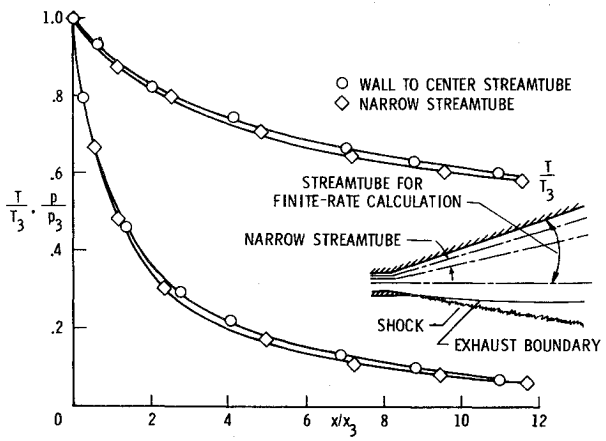

Fig. 1 Finite rate expansions in two streamtubes, $M_\infty = 6$.

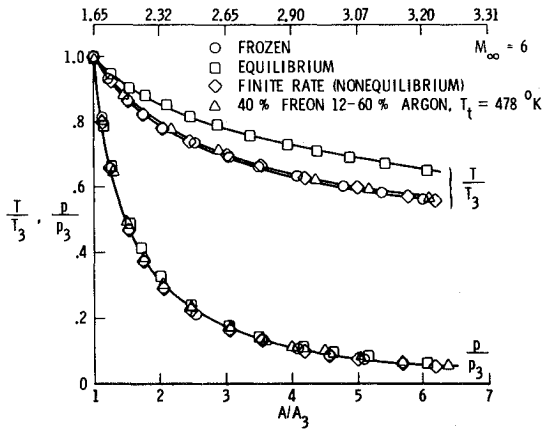

Fig. 2 Calculated pressure, temperature distributions, $M_\infty = 6$.

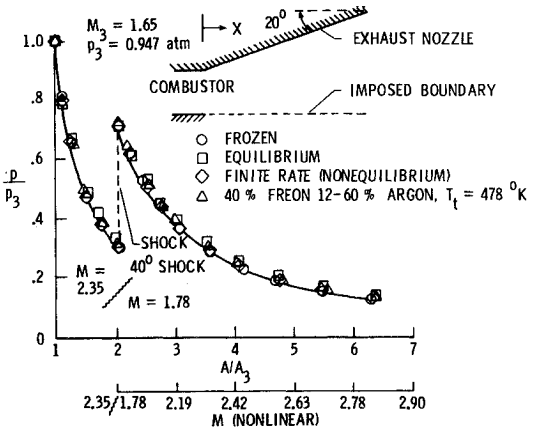

Fig. 3 Calculated pressure distribution with shock, $M_\infty = 6$.

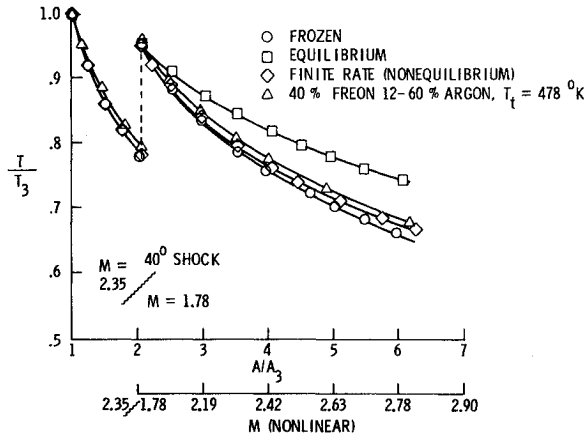

Fig. 4 Calculated temperature variation with shock, $M_\infty = 6$.

trends are essentially the same, the larger tube, more representative of the overall nozzle flowfield, was selected for this study.

State of the Flow

The state of the flow was determined by comparing the pressure, temperature, and isentropic exponent distributions for finite-rate, frozen, and equilibrium expansions at Mach 6 flight conditions. The pressure and temperature distributions are shown in Fig. 2 as a function of area ratio. Included are results for an equilibrium expansion of a simulant gas mixture (40% freon 12/60% argon, $T_t = 478$ K). The agreement between the pressure and temperature distributions for the frozen and finite-rate expansions, and the marked deviation of the equilibrium expansion, indicate that the nozzle flow is essentially frozen for the Mach 6 flight condition. The isentropic exponent distributions (not shown) displayed the same trend. Similar results were obtained for a Mach 8 flight case. The agreement between the simulant gas and the predicted distributions for the Mach 6 case provide encouragement that this technique can be used to simulate the exhaust flows of scramjet propulsion systems accurately.

Shock Discontinuities

The capability of the substitute gas simulation technique to predict the static distributions in shock-free scramjet nozzle flows accurately was shown in the preceding. The question arises as to the ability of the technique to predict the expansion properties behind an embedded shock. Since the exhaust flow is essentially frozen, an examination was made by expanding the flow in a frozen state and introducing a shock at a given area ratio. This shock represents one that could have been induced by overexpansion, off-design, or could emanate from the combustor or from the trailing edges of adjacent modules. The increase in temperature and pressure behind such a shock might shift the state of the expansion from frozen to equilibrium and limit the capability of the substitute gas to track the postshock flow.

A frozen shock crossing procedure was incorporated into the streamtube code. This option was used to generate the conditions behind the shock, which in turn were used as starting conditions for the postshock expansion. Results of this study are shown in the pressure and temperature distributions of Figs. 3 and 4, again for a Mach 6 flight case. As shown, a 40° shock was placed in the flow at an area ratio of 2 ($M = 2.35$). The postshock expansion remains frozen, as indicated by the close agreement between the frozen and finite-rate calculations. As before, the isentropic exponent distribution supported these results. The substitute gas also retains its ability to track the static distributions behind the shock. The shock strength was increased up to the point at which the postshock flow becomes subsonic (shock angle of approximately 50°) for Mach 6 flight conditions without departures from frozen flow. Similar results were obtained for Mach 8 flight conditions.

Concluding Remarks

A streamtube analysis of 2-D scramjet exhaust at Mach 6 and 8 flight conditions and a simulation technique employing substitute gas mixtures indicated the following results:

1) The scramjet exhaust flow is essentially frozen throughout the expansion at Mach 6 and Mach 8.

2) The flow behind shocks of moderate strength remains frozen.

3) The substitute gas simulation technique can track the static distributions accurately in scramjet exhaust flows (with and without shocks).

References

[1] Edwards, C.L.W., Small, W. J., Weidner, J. P., and Johnston, P. J., "Studies of Scramjet/Airframe Integration Techniques for Hypersonic Aircraft," AIAA Paper 75-78, Jan. 1975.

[2] Small, W. J., Weidner, J. P., and Johnston, P. J., "Scramjet Nozzle Design and Analysis as Applied to a Highly Integrated Hypersonic Research Airplane," NASA TM X-71972, Nov. 1974.

[3] Hunt, J. L., Talcott, N. A. Jr., and Cubbage, J. M., "Scramjet Exhaust Simulation Technique for Hypersonic Aircraft Nozzle Design and Aerodynamic Tests," AIAA Paper 77-83, Jan. 1977.

[4] Oman, R. A., Foreman, K. M., Leng, J., and Hopkins, H. B., "Simulation of Hypersonic Scramjet Exhaust," NASA CR-2494, March 1975.

[5] Salas, M. D., "Shock Fitting Method for Complicated Two-Dimensional Supersonic Flows," *AIAA Journal*, Vol. 14, May 1976, pp. 583-588.

[6] Lordi, J. A., Mapes, R. E., and Moselle, J. R., "Computer Program for the Numerical Solution of Nonequilibrium Expansions of Reacting Gas Mixtures," NASA CR-472, May 1966.

[7] Glowack, W. J. and Anderson, J. D. Jr., "A Computer Program for CO_2-N_2-H_2O Gasdynamic Laser Gain and Maximum Available Power," Naval Ordnance Laboratory, NOLTR 71-210, Oct. 1971.

Comparative Flutter Calculations for the Viggen Aircraft

Valter J. E. Stark*
Saab-Scania AB, Linköping, Sweden
and
Dale E. Cooley†
Wright-Patterson Air Force Base, Ohio

THE canard wing configuration of the Saab-Scania Viggen aircraft is interesting for the aeroelastician since three-dimensional effects and interference effects should be taken into account. Two comparative flutter calculations by different methods, but based on the same ground vibration test data, have been carried through for this configuration. One of the calculations was conducted by Saab-Scania and the other by the U.S. Air Force Flight Dynamics Laboratory (FDL).

In the two calculations, which were limited to the subsonic Mach number range and symmetric oscillations, the same idealized geometric shape was used. This consists of four pairs of trapezoidal panels S_1, S_2, S_3, and S_4, which are shown in Fig. 1. The deflection was approximated by a linear combination of five elastic modes plus the rigid translation and pitch modes. The former are characterized as follows:

1)	Wing bending	with frequency ω_1'
2)	Body bending	with frequency $1.40\omega_1'$
3)	Engine mode	with frequency $1.86\omega_1'$
4)	Wing torsion	with frequency $2.48\omega_1'$
5)	Motion in wing plane	with frequency $2.59\omega_1'$

The elastic modes contain contributions from control-surface deflections; but for the low-order modes considered, these are not significant ($\omega_1' = 8.63$ Hz).

Since the aerodynamic control points do not coincide with the ground vibration test points and since the streamwise slope of the deflection is also needed, interpolation was required. In the FDL calculation, this was achieved by using a grid of spanwise and chordwise lines connecting node points at which modal deflections were specified. The deflections were interpolated along the spanwise lines to each station at which aerodynamic control points lie, and then interpolated chordwise to the aerodynamic control point. An interpolation formula was used to determine a cubic polynomial function for the approximation. In cases for which the modal deflection is specified at more than four points spanwise or chordwise, the approximation is a piecewise-continuous cubic polynomial.

In the SAAB calculation, linear combinations of given functions of two variables were fitted by the method of least squares to the measured modal deflections.[1] One combination was determined for each panel. The given functions are products of chordwise and spanwise factors. These are special polynomials with vanishing second- and third-order derivatives at free panel edges, which yields appropriate behavior of the resulting analytic modes. Control-surface deflections can be treated if needed by including discontinuous deflection functions (see Fig. 11 of Ref. 1).

The aerodynamic forces were obtained in the FDL calculation by means of the Doublet Lattice Method[2] and a computer program based on Ref. 3. The boxes considered in this method are formed by the common area of chordwise and spanwise strips. The panels S_1, S_2, S_3, and S_4 contained 6, 6, 4, and 6 chordwise strips and 5, 10, 8, and 6 spanwise strips, respectively. The spanwise strips are formed by constant percent chord lines. The box dimensions decrease in the outboard direction to keep the box aspect ratio approximately constant and near unity. The resulting number of boxes on one half of the configuration amounted to 158.

In early flutter calculations[4] at Saab-Scania for the Viggen aircraft, the aerodynamic forces were generated by computer programs based on the Lifting Line Element principle, which was discussed and exemplified in Ref. 5 and which also forms the basis of the Doublet Lattice Method. In this calculation, however, a new Fortran program system based on the Polar Coordinate Method[6] has been used. The jump in the advanced velocity potential[7] is approximated in this method by a linear combination of given potential jumps. Like the functions in the combination for the deflection, these jumps are partly products of simple chordwise and spanwise factors (integrals of Birnbaum-Glauert functions) and partly special jumps.[8] The coefficients of the special jumps, which correspond to the discontinuous deflection functions, are known, whereas those of the simple jumps are to be solved from a set of linear equations. The matrix of this set is obtained by considering the velocity field that corresponds to each given potential jump and by calculating the normal component of the field at appropriate control points.

This calculation is performed by subtracting the kernel function singularity by means of a first-order polynomial, which at least in the steady case can be said to be a tangent plane[9] to the potential jump, and by employing polar integration variables. The formulation implies that the normal velocity component does not ordinarily appear as a difference between large numbers,[9] and that those integrals, which must be evaluated numerically, receive well-behaved integrands.[9] The velocity field that corresponds to a given potential jump is independent of the deflection mode, and the matrix of the

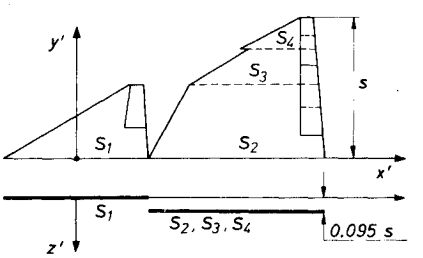

Fig. 1 Idealized Viggen configuration.

Received March 14, 1977; revision received May 9, 1977.
Index categories: Aeroelasticity and Hydroelasticity; Nonsteady Aerodynamics.

*Research Scientist, Aerospace Division. Member AIAA.
†Technical Manager, Aeroelastic Group, U.S. Air Force Flight Dynamics Laboratory. Member AIAA.